
On Calibration and Out-of-domain Generalization

Yoav Wald*
 Hebrew University
 yoav.wald@gmail.com

Amir Feder*
 Technion
 amirfeder@gmail.com

Daniel Greenfeld
 Jether Energy Research
 danielgreenfeld3@gmail.com

Uri Shalit
 Technion
 urishalit@technion.ac.il

Abstract

Out-of-domain (OOD) generalization is a significant challenge for machine learning models. To overcome it, many novel techniques have been proposed, often focused on learning models with certain invariance properties. In this work, we draw a link between OOD performance and model calibration, arguing that calibration across multiple domains can be viewed as a special case of an invariant representation leading to better OOD generalization. Specifically, we prove in a simplified setting that models which achieve multi-domain calibration are free of spurious correlations. This leads us to propose multi-domain calibration as a measurable surrogate for the OOD performance of a classifier. An important practical benefit of calibration is that there are many effective tools for calibrating classifiers. We show that these tools are easy to apply and adapt for a multi-domain setting. Using five datasets from the recently proposed WILDS OOD benchmark [23] we demonstrate that simply re-calibrating models across multiple domains in a validation set leads to significantly improved performance on unseen test domains. We believe this intriguing connection between calibration and OOD generalization is promising from a practical point of view and deserves further research from a theoretical point of view.

1 Introduction

Recent improvements in the design of machine learning systems have led to impressive results in a plethora of fields [20, 10, 42]. However, as models are typically only trained and tested on in-domain data, they often fail to generalize to out-of-domain (OOD) data [23]. The problem is amplified when deploying such systems in the wild, where they are required to perform well under conditions that might not have been observed during training. For instance, a medical diagnosis system trained on patient data from a few hospitals could fail when deployed in a new hospital with different patient demographics or infrastructure.

Many methods have been proposed to improve the OOD generalization of machine learning models. Specifically, there is a rapidly growing interest in learning models that are invariant to distribution shifts and do not rely on spurious correlations in the training data [35, 18, 1]. Such attempts highlight the need for learning robust models with invariance properties, but have demonstrated limited success in scaling to realistic high-dimensional data, and in learning invariant representations [38, 21].

In this paper, we argue that an alternative approach for learning invariant representations could be achieved through model calibration. Calibration asserts that the probabilities of outcomes predicted by a model match their true probabilities. Our claim is that simultaneous calibration over several

*Equal contribution

domains can be used as an observable indicator for favorable performance on unseen domains. For example, if we take all cases where a classifier outputs a probability of 0.9 that patients are ill, and in one hospital the true probability of illness in these cases is 0.85 while in the other it is 0.95, then we may suspect it relies on spurious correlations. Intuitively, the features which lead the classifier to predict a probability of 0.9 imply different results under different experimental conditions, suggesting that their correlation with the label is unstable. Conversely, if the true probabilities in both hospitals match the classifier’s output, it may be a sign of its robustness. Here, we attempt to formalize this intuition and demonstrate its validity on real data.

Concretely, let $X \in \mathcal{X}$ be the features, Y the labels and E the domains (or environments) [35]. We assume the data generating process for E, X, Y follows the causal graph in Fig. 1, and that some parts of X are causal and others anti-causal. We differentiate between the anti-causal variables X which are affected and unaffected by E , denoted as $X_{\text{ac-spurious}}$ and $X_{\text{ac-non-spurious}}$, respectively. We do not assume to know how to partition X into X_{causal} , $X_{\text{ac-spurious}}$, $X_{\text{ac-non-spurious}}$. The main assumptions made in the causal graph in Fig. 1 are that there are no hidden variables, and that there is no edge directly from environment E to the label Y . If such an arrow exists, it implies the conditional distribution of Y given X can be arbitrarily different in an unseen environment E , compared to those present in the training set. Note that for simplicity we do not include arrows from X_{causal} to $X_{\text{ac-spurious}}$ and $X_{\text{ac-non-spurious}}$ but they may be included as well.

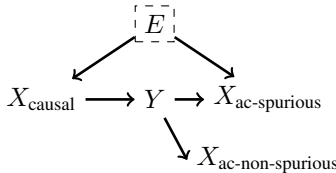


Figure 1: Learning in the presence of causal and anti-causal features. Anti-causal features can be either spurious ($X_{\text{ac-spurious}}$), or non-spurious ($X_{\text{ac-non-spurious}}$).

Generally, a representation $\Phi(X)$ contains a *spurious correlation* with respect to the environments E and label Y , if $Y \not\perp\!\!\!\perp E \mid \Phi(X)$. Similar observations have been made by [18, 1]. Having a spurious correlations thus implies that the relation between Φ and the target variable depends on the environment – it is not transferable or stable across environments. Note that “spuriousness” is with respect to the environment random variable E , so the same representation might be spurious with respect to one set of environments and not another.

For binary Y , if we take our representation to simply be the output $f(X)$ of classifier $f : \mathcal{X} \rightarrow [0, 1]$, then a classifier with no spurious correlation w.r.t. E satisfies $Y \perp\!\!\!\perp E \mid f(X)$. The crux of this paper is the observation, proven in 2.3, that this conditional independence implies that up-to a simple transformation, $\mathbb{E}[Y \mid f(X), E = e] = f(X)$ for every value of E , which in turn is equivalent to stating “ f is a **calibrated** classifier across all environments”.

In the following sections, we crystallize this observation. First, we prove in a Gaussian-linear setting, under a general-position condition, that indeed being calibrated across a sufficient number of environments implies the model has no spurious correlations. Then, we demonstrate on the WILDS benchmark datasets [23] that simply re-calibrating models across multiple environments, improves performance on unseen environments. Finally, we show on the colored MNIST dataset [22] that multi-domain calibration is a useful measure for model selection.

2 Calibration and Invariant Classifiers

2.1 Problem Setting

Consider observable features X , a label Y and an environment E with sample spaces $\mathcal{X}, \mathcal{Y}, \mathcal{E}$ accordingly. In this work we mostly focus on the tasks of regression and binary classification, therefore $\mathcal{Y} = \mathbb{R}$ or $\mathcal{Y} = \{0, 1\}$. To lighten notation, our definitions will be given for the binary classification setting and we will point out adjustments to regression where necessary. There is no explicit limitation on $|\mathcal{E}|$, but we do observe training data that has been collected from a certain finite subset of the possible environments $\mathcal{E}_{\text{train}} \subset \mathcal{E}$. The number of training environments is

denoted by k , and $E_{\text{train}} = \{e_i\}_{i=1}^k \subset \mathcal{E}$, so that our training data is sampled from a distribution $P[X, Y | E = e_i] \quad \forall i \in [k]$. The scope of our formal discussion will be limited to the population setting, hence we do not introduce notation for the datasets collected from each environment. We will refer to the range of f upon limiting its domain to the support of $P[X | E = e_i]$, as the range of f restricted to e_i . When taking expectations and conditional expectations over distributions, we will drop the subscripts whenever they are clear from context (e.g. write $\mathbb{E}[\cdot | E = e_i]$ instead of $\mathbb{E}_{\mathbf{x}, y \sim P[X, Y | E = e_i]}[\cdot]$).

Our goal is to learn a predictor $f : \mathcal{X} \rightarrow [0, 1]$ and evaluate its risk with respect to a loss function $l : \mathcal{Y} \times [0, 1] \rightarrow \mathbb{R}$. Ideally, we would like to learn a classifier that is optimal for all environments \mathcal{E} . Unfortunately, we only observe data from the limited set E_{train} and even if this set is extremely large, the Bayes optimal classifiers on each environment do not coincide. Many techniques for OOD generalization thus focus on minimizing the worst-case risk over \mathcal{E} :

$$\min_f \max_{e \in \mathcal{E}} \mathbb{E}[l(y, f(\mathbf{x})) | E = e]. \quad (1)$$

Prominent examples include Distributionally Robust Optimization (DRO) [40, 4], Graph Surgery [44], Invariant Causal Predictions [35] and Invariant Risk Minimization (IRM) [1].

In what follows, we discuss why models that are well-calibrated on all training environments have high potential for good OOD performance. Intuitively, calibration imposes high quality uncertainty estimates for each $e \in \mathcal{E}$ [15]. It turns out that under certain conditions, this property helps $f(X)$ discard $X_{\text{ac-spurious}}$ as viable features for prediction. A condition that is often necessary in order to provide meaningful bounds on Equation (1).

2.2 Calibration Across Multiple Environments

A classifier is calibrated if it delivers accurate uncertainty estimates for its prediction. The following definition states this formally for binary classification problems, along with a straightforward generalization to the case with multiple training environments, which demands calibration for each environment separately.

Definition 1 *Let $f : \mathcal{X} \rightarrow [0, 1]$ and $P[X, Y]$ be a joint distribution over the features and label. Then $f(\mathbf{x})$ is calibrated w.r.t to P if for all $\alpha \in [0, 1]$ in the range of f :*

$$\mathbb{E}_P[Y | f(X) = \alpha] = \alpha.$$

In the multiple environments setting, $f(\mathbf{x})$ is calibrated on E_{train} if for all $e_i \in E_{\text{train}}$ and α in the range of f restricted to e_i :

$$\mathbb{E}[Y | f(X) = \alpha, E = e_i] = \alpha.$$

For regression problems, we consider regressors that output estimates for the mean and variance of Y , and say they are calibrated if they match the true values similarly to the definition above. The precise definition can be found in the supplementary material.

2.3 Invariance and Calibration on Multiple Domains

To tie the notion of calibration on multiple environments with OOD generalization, we start by noting its correspondence with our definition of spurious correlations. Recall the definition that a representation $\Phi(X)$ does not contain spurious correlations if $Y \perp\!\!\!\perp E | \Phi(X)$. Treating the output of a classifier as a representation of the data, i.e. $\Phi(X) = f(X)$, and considering classifiers which satisfy this conditional independence with respect to training environments, we arrive at a definition of an invariant classifier.

Definition 2 *Let $f : \mathcal{X} \rightarrow [0, 1]$, it is an invariant classifier w.r.t E_{train} if for all $\alpha \in [0, 1]$ and environments $e_i, e_j \in E_{\text{train}}$ where α is in the range of f restricted to each of them:*

$$\mathbb{E}[Y | f(X) = \alpha, E = e_i] = \mathbb{E}[Y | f(X) = \alpha, E = e_j]. \quad (2)$$

We now show the correspondence between invariant classifiers and classifiers calibrated on multiple environments:

Lemma 1 A binary classifier is invariant w.r.t E_{train} if and only if there exists a function $g : \mathbb{R} \rightarrow [0, 1]$ such that $g \circ f$ is calibrated on all training environments.

Proof Assume that the classifier is invariant and let $\hat{\alpha} \in \mathbb{R}$ be any value in the range of f . Due to invariance, for all $e_i \in E_{\text{train}}$ where $\hat{\alpha}$ is in the range of f restricted to e_i , there must exist $\alpha \in [0, 1]$ such that $\mathbb{E}[Y | f(X) = \hat{\alpha}, E = e_i] = \alpha$. Setting $g(\hat{\alpha}) = \alpha$ results in a classifier $g \circ f$ that is calibrated on E_{train} . Conversely, if a classifier is calibrated on all E_{train} , then setting g to the identity function shows it is also invariant w.r.t E_{train} . \blacksquare

Now, we can note how the above notion of invariance relates to that of IRM, where invariance is linked to the optimality of a classifier.

Definition 3 [1] $\Phi : \mathcal{X} \rightarrow \mathcal{H}$ elicits an invariant classifier if there exists $\mathbf{w}^* : \mathcal{H} \rightarrow \mathbb{R}$ that satisfies simultaneously for all $i \in [k]$ that $\mathbf{w}^* \in \arg \min_{\mathbf{w}} \mathbb{E}[l(Y, \mathbf{w} \circ \Phi(X)) | E = e_i]$.

When the loss function is either the squared or logistic loss, they show that $\Phi(X)$ elicits an invariant predictor if and only if for all $h \in \mathcal{H}$ and $i, j \in [k]$:

$$\mathbb{E}[Y | \Phi(X) = h, E = e_i] = \mathbb{E}[Y | \Phi(X) = h, E = e_j].$$

This coincides with Equation (2) when taking $\Phi(X) = f(X)$. On the other hand, calibration does not impose any kind of risk minimization, which means that this property does not depend on the choice of a loss function. Having established the connection between calibration on multiple environments and invariance, there are several interesting questions and points that arise.

Generalization. Suppose that $f(X)$ is calibrated on E_{train} . Under what conditions does this imply it is calibrated on \mathcal{E} ? For instance, it is easy to show that calibration on several environments entails calibration on any distribution which can be expressed as a linear combination of the distributions underlying said environments. Yet in general, given a set \mathcal{E} we would like to know how many and what kind of training environments are required for calibration to generalize.

Dependence on $X_{\text{ac-spurious}}$. To give any kind of useful bound on the worst-case risk in Equation (1), it is usually required to guarantee $f(X)$ does not use $X_{\text{ac-spurious}}$ to produce its predictions. Thus, in order to claim that calibration is correlated with good OOD performance, we should also show if and when it delivers such a guarantee.

Calibration and Sharpness. Calibration alone is not enough to guarantee that a classifier performs well; on a single environment, always predicting $\mathbb{E}[Y]$ will give a perfectly calibrated classifier. Hence, calibration should be combined with some sort of guarantee on accuracy. In the calibration literature, this is often referred to as sharpness. That said, calibration can guarantee that the classifier “fails gracefully” in the sense that its accurate uncertainty estimates inform us whenever it is expected to incur high error. Our work leaves much to be explored in this area; nonetheless, in the experimental part we will discuss simple ways to control the trade-off between calibration and sharpness when working with pre-trained models.

3 Motivation: a Linear-Gaussian Model

Let us consider data where X is a multivariate Gaussian. Since we will be considering Gaussian data, the set of all environments \mathcal{E} will be parameterized using pairs of real vectors expressing expectations and positive definite matrices of an appropriate dimension expressing covariances: $\mathcal{E} = \{(\mu, \Sigma) \mid \mu \in \mathbb{R}^d, \Sigma \in \mathbb{S}_{++}^d\}$.

For two scenarios (a and b in Figure 2) we prove that when provided with data from k training environments, where k is linear in the number of features, and the environments satisfy some mild non-degeneracy conditions, any predictor that is calibrated on the training environments will also be calibrated on all $e \in \mathcal{E}$ and will not rely on any of the spurious features $X_{\text{ac-sp}}$.

In the first scenario, Y is a binary variable drawn from a Bernoulli distribution with parameter $\eta \in [0, 1]$, and observed features are generated conditionally on Y . $\mathbf{x}_{\text{ac-ns}} \in \mathbb{R}^{d_{\text{ns}}}$ features are invariant in the sense that their conditional distribution given Y is the same for all environments; $\mathbf{x}_{\text{ac-sp}} \in \mathbb{R}^{d_{\text{sp}}}$ features are spurious as their distribution may shift between environments, altering their correlation with Y . The data generating process, depicted in Figure 2a for training environment $i \in [k]$ is thus given by:

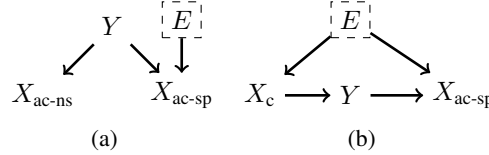


Figure 2: Graphs describing the two cases in our theoretical analysis. We use acronyms in the subscripts to lighten notation. (a) All features are anti-causal, some are spurious while others are invariant. (b) Features are either causal and may undergo covariate shift, or are anti-causal and spurious.

$$y = \begin{cases} 1 & \text{w.p } \eta \\ -1 & \text{o.w} \end{cases} \quad \begin{aligned} X_{\text{ac-ns}} \mid Y = y &\sim \mathcal{N}(y\mu_{\text{ns}}, \Sigma_{\text{ns}}), \\ X_{\text{ac-sp}} \mid Y = y &\sim \mathcal{N}(y\mu_i, \Sigma_i). \end{aligned} \quad (3)$$

We consider a linear classifier $f(\mathbf{x}; \mathbf{w}, b) = \sigma(\mathbf{w}^\top \mathbf{x} + b)$.

The function $\sigma : \mathbb{R} \rightarrow [0, 1]$ is some invertible function (e.g. a sigmoid) that turns the results of the affine transformation into an estimate of Y . Since the mean of spurious features, μ_i , is determined by y , these features can help predict the label in some environments. Yet, these correlations do not carry to all environments, and $f(\mathbf{x})$ can thus absorb spurious correlations whenever the coefficients in \mathbf{w} corresponding to $X_{\text{ac-sp}}$ are non-zero. In terms of the worst-case risk of Equation (1), the only way to provide a meaningful bound is to have all of these coefficients set to 0, since otherwise a new environment can reverse and magnify the correlations observed on E_{train} . Using these definitions, we may now state our result for this case:

Theorem 1 *Given $k > 2d_{\text{sp}}$ training environments where data is generated according to Equation (3) with parameters $\{\mu_i, \Sigma_i\}_{i=1}^k$, we say they lie in general position if for all non-zero $\mathbf{x}_{\text{ac-sp}} \in \mathbb{R}_{\text{sp}}^d$:*

$$\dim \left(\text{span} \left\{ \begin{bmatrix} \sum_i \mathbf{x}_{\text{ac-sp}} + \mu_i \\ 1 \end{bmatrix} \right\}_{i \in [k]} \right) = d_{\text{sp}} + 1.$$

If a linear classifier is calibrated on k training environments which lie in general position then its coefficients for spurious features are zero. Moreover, the set of training environments that do not lie in general position has measure zero in the set of all possible training environments \mathcal{E}^k .

As a corollary, we see that calibration on training environments generalizes to calibration on \mathcal{E} . The proof of this theorem is given in the supplementary material and uses similar tools to the proof of Theorem 10 in [1]. The data generating process closely resembles the one considered by [38], who use diagonal covariance matrices. In the supplementary material we also show that in their setting, calibration requires 1 more environment than IRM to discard spurious correlations. This matches the intuition where training environments reduce degrees of freedom from the space of invariant classifiers, and then risk minimization reduces an additional one.

In the second scenario we consider, alongside the spurious features there are causal features subject to covariate shift $\mathbf{x}_c \in \mathbb{R}^{d_c}$, as shown in Figure 2b. The covariate shift is induced when the environments E alter the distribution of the causal features \mathbf{x}_c [41]. In this case, we analyze a regression problem since it is amenable to exact analysis. The data generating process we consider for training environment $i \in [k]$ is:

$$\begin{aligned} X_c &\sim \mathcal{N}(\mu_i^c, \Sigma_i^c); Y = \mathbf{w}_c^{*\top} \mathbf{x}_c + \xi, \xi \sim \mathcal{N}(0, \sigma_y^2) \\ X_{\text{ac-sp}} &= y\mu_i + \eta, \eta \sim \mathcal{N}(\mathbf{0}, \Sigma_i). \end{aligned} \quad (4)$$

In this case, to give a meaningful bound on Equation (1), it is not enough for $f(X)$ to ignore $X_{\text{ac-sp}}$, it should also capture \mathbf{w}_c^* since it characterizes $P(Y \mid X_{\text{causal}})$, which is the invariant mechanism in this scenario². Interestingly, it turns out that calibration on multiple domains, without imposing risk minimization, can retrieve the correct solution.

²An explicit bound on the worst-case risk would require an additional assumption on the variances of the causal features, but we refrain from deriving it here since we are more interested in capturing the invariant parameters.

Theorem 2 (informal) Let $f(\mathbf{x}; \mathbf{w}) = \mathbf{w}^\top \mathbf{x}$ be a linear regressor and assume we have $k > \max\{d_c + 2, d_{sp}\}$ training environments where data is generated according to Equation (4). Under mild non-degeneracy conditions, if the regressor is calibrated across all training environments then the coefficients corresponding to X_c equal \mathbf{w}_c^* and those that correspond to X_{ac-sp} are zero.

In the supplementary material we give the exact form of non-degeneracy condition that is required here, which has a similar flavor to the one in Theorem 1.

Taken together, the results presented here show that calibration can generalize across environments given that the number of environments is approximately the number of spurious features. They also show that for the simple settings considered here, calibration implies avoiding spurious correlation. The results are of the same type shown in works like [1, 38], but with the notable difference that they do not directly refer to risk minimization. Hence they do not include an assumption about the loss being used at the learning stage. Instead, they rely on a relatively stable and well-known notion of calibration, albeit over multiple environments.

Considering the large volume of recent work that is dedicated to invariance and learning under distribution shifts, we now turn to discuss some of them in the context of this paper. The valuable insights gained from this literature motivates us to examine what type of value can calibration bring.

4 Related Work

As discussed in Section 2, multi-domain calibration is an instance of an invariant representation. Following [1], many extensions have been proposed, e.g. [24, 3]. Yet, recent work claims that many of these approaches still fail to find invariant relations in some cases of interest [21, 38, 14], where a significant challenge seems to be the gap between what is achieved by the regularization term used in practice and the goal of conditional independence $Y \perp\!\!\!\perp E \mid \Phi(X)$. [12] give a sobering view on methods for OOD generalization, emphasizing the power of ERM and data augmentation, and the challenge of model selection. We claim that the multi-domain calibration studied here is a somewhat simpler form of invariance. Calibration is attractive because there are standard tools to quantify it such as calibration scores [33], and calibration might sometimes be achieved even with post processing.

Learning models which generalize OOD is a fruitful area of research that has seen many recent developments. Most work focuses on the case where unlabeled samples are available from the target domain, including recent work on OOD calibration where unlabeled samples from the target domain are available [47]. However, important work has also been done on the area of our focus – the so-called “proactive” case [44], where no OOD samples are available whatsoever [29, 18, 39, 35, 40]. Since calibration can be applied easily to any model, it can be interesting to see whether it proves beneficial for models trained using different approaches to achieve OOD generalization.

Calibration also plays an important role in uncertainty estimation for deep networks [13], and recently in fairness, where calibration on subgroups of populations is sought [37]. This has interesting resemblance to the multiple environments calibration we consider here. A more general notion of multi-calibration has also been studied in this context [17], with recent results on sample complexity [43] which may provide tools that carry over to finite sample analysis of domain generalization. Finally, methods for training calibrated models [26] might be generalized to the multiple environment scenario and this is an interesting direction for future work. Still, in this work we focus on working with pre-trained models, using methods that we now turn to describe.

5 Calibration and Model Selection Methods

Two valuable tools to assess calibration of a model are *calibration plots* and scalar summaries such as the Expected Calibration Error, known as the *ECE score*.

Calibration plots [8] are a visual representation of model calibration in the case of binary labels. Each example \mathbf{x} is placed into one of B bins that partition the $[0, 1]$ interval, in which the output, or *confidence*, of the classifier $f(\mathbf{x})$ falls. For each bin b , the accuracy of f on the bin’s examples $acc(b)$ is calculated along with the average confidence $conf(b)$. These are plotted against each other to form a curve, where deviations from a diagonal represent miscalibration.

ECE score is one common scalar summary of the calibration curve, calculated by averaging the

deviation between accuracy and confidence:

$$ECE = \sum_{b=1}^B \frac{n_b}{N} |acc(b) - conf(b)|. \quad (5)$$

n_b is the number of predictions in bin b , N is the total number of data points.

The main part of our experimental evaluation examines post-processing calibration techniques. We examine whether the extremely simple and computationally cheap act of calibrating a model can have an effect on OOD accuracy. The other part examines the use of calibration scores for model selection. As recently discussed by [12], model selection is non-trivial when the goal is OOD generalization. They show that suboptimal model selection can eliminate the advantage that techniques designed for OOD generalization have over ERM with data augmentation. As most model selection methods are based on accuracy, we consider a method based on the ECE score instead.

5.1 Post Processing Calibration

Binary classifiers are often calibrated using Platt Scaling [36] or Isotonic Regression Scaling [49, 32]. For our experiments we compared these and several other techniques using the ECE score they achieve [30]. We wound up using Isotonic Regression as it usually outperformed the alternatives. The input to the method is a dataset $(f_i, y_i)_{i=1}^N$, where f_i is a shorthand for the prediction of the model $f(\mathbf{x})$ on the i -th datapoint and y_i is the label. Isotonic Regression learns a *monotonic* mapping $z : \mathbb{R} \rightarrow \mathbb{R}$ solving:

$$(ISO) \quad \arg \min_z \frac{1}{N} \sum_{i=1}^N (z(f_i) - y_i)^2.$$

Unlike standard calibration problems, we have multiple domains to calibrate over. In our experiments (Section 7) we compare two methods for multi-domain calibration: naive calibration and distributionally robust calibration.

Naive Calibration takes predictions of a trained model f on validation data pooled from all domains and fits an isotonic regression z^* . We then report the performance of $z^* \circ f$ on the OOD test set. **Robust Calibration.** In a multiple domain setting, Naive calibration may produce a model that is well calibrated on the pooled data, but uncalibrated on individual environments. Motivated by the goal of simultaneous calibration, we offer the following alternative where we attempt to bound the worst-case miscalibration across environments. For each environment $e \in E_{\text{train}}$, we denote the number of validation examples we have from it by N_e , and by $f_{e,i}$ the prediction of the model on the i -th example. Then in a similar vein to robust optimization, robust isotonic regression solves:

$$z^* = \arg \min_z \max_{e \in E_{\text{train}}} \frac{1}{N_e} \sum_{i=1}^{N_e} (z(f_{e,i}) - y_i)^2. \quad (6)$$

Since Isotonic Regression can be cast as a Quadratic Program, and Equation (6) minimizes a pointwise maximum on similar objectives, we can cast it as a convex program and solve with standard optimizers. In our implementation we use CVXPY [11]. We then evaluate the OOD performance of $z^* \circ f$.

5.2 Calibration Scores for Model Selection

Algorithm 1 Model Selection with Worst-Case ECE

Input: Validation sets $\{(\mathbf{X}_i, \mathbf{y}_i)\}_{i=1}^k$, Models $\{f_j(\mathbf{x})\}_{j=1}^L$

Output: Selected model $f^*(\mathbf{x})$

Pool data from all environments to (\mathbf{X}, \mathbf{y})

for $j \in [L]$ **do**

$z_j \leftarrow ISO(f_j(\mathbf{X}), \mathbf{y})$

for $i \in [k]$ **do**

$ECE_{i,j} \leftarrow ECE$ of $z_j \circ f_j$ on $(\mathbf{X}_i, \mathbf{y}_i)$

 Return f_j for $j \in \arg \min_j \max_i ECE_{i,j}$

The model selection procedure we examine takes L pretrained models on k training environments, along with validation sets for each environment. As described in Algorithm 1 it selects a model based on the best worst-case ECE over environments. We follow [30] and calibrate each model before calculating the ECE. This is important since ECE can be very high on models that actually become well calibrated upon simple post-processing.

6 Experimental Setup

6.1 WILDS Benchmarks

Dataset	Type	Label (y)	Input (x)	Domain (d)	Model ($f(x)$)
PovertyMap	Regression	Asset Wealth Index	Satellite Image	Country	ResNet
Camelyon17	Binary	Tumor Tissue	Histopathological Image	Hospital	DenseNet
CivilComments	Binary	Comment Toxicity	Online Comment	Demographics	BERT
FMoW	Multi-class	Land Use Type	Satellite Image	Region	DenseNet
AmazonReviews	Binary	Sentiment	Product Review	Product Area	Random Forest

Table 1: Description of each of the datasets used in our WILDS experiments.

WILDS is a recently proposed benchmark of in-the-wild distribution shifts from several data modalities and applications. Table 1 presents the five WILDS datasets we experiment with, chosen to represent different OOD generalization scenarios. We use the models and training algorithms proposed by [23]. In order to perform multi-domain calibration we modify the data to include a multi-domain validation set whenever possible.³

Models and Algorithms. In four of the five WILDS experiments, we use models with the same implementation as presented by [23]. In the AmazonReviews experiments, we test different models and report results on the Random Forest classifier (see supp. mat. for results on the others). As in [23], we use four different training algorithms to train our models: **ERM**, **IRM**, **DeepCORAL** and **GroupDRO**. For each of the CivilComments, Camelyon17, FMoW and PovertyMap experiments, we train and compare three different training algorithms. We train each model four times using a different random seed, and report the average results and their standard deviations.

6.2 Colored MNIST

Colored MNIST is a variant of the classical MNIST dataset [27], where a color bias was planted into each digit [22]. We use it to test the efficacy of using calibration measures for model selection, choosing hyperparameters for an IRM trained multilayer perceptron over 25 restarts. In their experiments [1] perform model selection by measuring error on data taken from the test environment, which is undesirable in practice. Our experiment serves as a proof of concept for calibration based model selection in such scenarios.

7 Results

Using the datasets, models and optimization algorithms presented in Section 6, we perform two sets of experiments demonstrating the usefulness of calibration for OOD performance. First, we employ five datasets from [23] and test the efficacy of the calibration methods proposed in Section 5 in improving the performance of state-of-the-art systems on unseen environments. Then, using Colored MNIST, we explore the possibility of using in-domain (ID) calibration for selecting models to perform on OOD data.

7.1 Calibration and OOD Performance

Results on the *PovertyMap* dataset, presented in Table 2 (top), show that calibration consistently improves OOD performance. Specifically, the robust calibration approach outperforms alternatives regardless of the training algorithm. Interestingly, it also leads to more stable results, as can be seen in the standard deviation across different model runs. Comparatively, the naive calibration approach has mixed results, demonstrating significant improvement in the IRM runs but no gains for ERM.

³See supp. mat. for a detailed description of the data and splits.

Table 2 (bottom) presents our results on the *Camelyon17* dataset, with similar patterns to those observed in *PovertyMap* (top). Notably, robust calibration is 0.5% better (absolute) than naive calibration, and 4.2% then the original model. The largest improvement was in the DeepCORAL experiments, where robust calibration improved OOD accuracy by 6.2% (absolute) compared to the original model.

Algorithm	<i>PovertyMap</i> ID	<i>PovertyMap</i> OOD		
		Orig.	Naive Cal.	Rob. Cal.
ERM	0.828 (0.018)	0.832 (0.011)	0.827 (0.014)	0.834 <u>(0.006)</u>
DeepCORAL	0.833 (0.009)	0.832 (0.011)	0.835 <u>(0.009)</u>	0.837 (0.012)
IRM	0.823 (0.012)	0.735 (0.117)	0.812 (0.016)	0.815 <u>(0.015)</u>

Algorithm	<i>Camelyon17</i> ID	<i>Camelyon17</i> OOD		
		Orig.	Naive Cal.	Rob. Cal.
ERM	94.81 (0.023)	66.66 (0.144)	71.23 (0.089)	70.93 <u>(0.086)</u>
DeepCORAL	96.1 (0.0006)	73.87 (0.041)	78.51 (0.025)	79.96 <u>(0.019)</u>
IRM	95.62 (0.029)	77.03 (0.059)	78.99 (0.058)	79.31 (0.06)

Table 2: Top: Pearson correlation r on in-domain (ID) and OOD (unseen countries) test sets in *PovertyMap*. Bottom: Accuracy on ID and OOD (unseen hospital) test sets in *Camelyon17*. Orig.: original algorithm with no changes applied. Best OOD result for each domain is highlighted in **bold**. Standard deviation across model runs in brackets, lowest OOD std. is underlined.

Observing the *CivilComments* results (Table 3), ERM’s performance is not improved substantially when calibrating it, but IRM is improved by 31.7% (absolute) after calibration. Interestingly, the very large variance observed in the IRM runs (0.199) is reduced by a factor of 16 after applying robust calibration (0.012). Looking at worst-case performance across demographic groups, we see calibration is very useful, improving performance by an average of 17.8%.

Table 4 presents results on the *FMoW* dataset. As this is a multi-class classification task, where calibration methods were shown to be less effective, differences between all approaches are substantially smaller. While the average performance does not substantially increase following the calibration post-process, it does significantly improve the worst-case performance for all training algorithms.

Finally, Table 5 presents the *AmazonReviews* results, where calibration improves OOD accuracy on all six domains. Moreover, in all experiments, the robust calibration approach outperforms the original model, with an average improvement of 0.3% (absolute) over naive calibration and more than 12.6% over the original model.

Analysis. In our experiments, calibrating a trained model usually improves OOD performance. Interestingly, when our post-processing does not improve OOD performance, it is often linked to our inability to improve ID calibration. As can be seen in Figure 3, there is a connection between ID calibration and OOD performance. Specifically, in the DeepCORAL experiments (top), robust

	Algorithm	Orig.	Naive Cal.	Rob. Cal.
Average	ERM	92.06 (0.004)	92.32 (0.004)	92.63 <u>(0.003)</u>
	IRM	55.74 (0.199)	87.21 (0.016)	87.47 <u>(0.012)</u>
	GroupDRO	89.35 (0.006)	92.18 (0.003)	92.56 <u>(0.001)</u>
Worst	ERM	62.09 (0.026)	76.38 <u>(0.005)</u>	79.93 (0.008)
	IRM	40.61 (0.16)	69.09 (0.013)	68.76 <u>(0.013)</u>
	GroupDRO	72.02 (0.004)	76.69 (0.013)	79.31 (0.007)

Table 3: Average (top) and worst-case (bottom) group accuracy on the test set in the *CivilComments* dataset.

		Algorithm	Orig.	Naive Cal.	Rob. Cal.
<i>Average</i>		ERM	52.98 (0.003)	53.01 (0.004)	52.83 (0.004)
		DeepCORAL	50.61 (0.003)	50.71 (0.003)	50.5 (0.003)
		IRM	50.72 (0.004)	51.05 (0.004)	50.92 (0.003)
<i>Worst</i>		ERM	32.63 (0.016)	33.09 (0.021)	37.19 (0.035)
		DeepCORAL	31.73 (0.01)	31.75 (0.01)	33.86 (0.016)
		IRM	31.33 (0.012)	31.81 (0.016)	34.41 (0.015)

Table 4: Average (top) and worst (bottom, region) accuracy on the OOD test set in *FMoW*.

Target Domain	ID	OOD		
		Orig.	Naive Cal.	Rob. Cal.
<i>DM</i>	0.674 (0.007)	0.609 (0.015)	0.599 (0.009)	0.614 (0.008)
<i>B</i>	0.647 (0.006)	0.520 (0.009)	0.603 (0.010)	0.630 (0.007)
<i>AV</i>	0.636 (0.011)	0.621 (0.014)	0.719 (0.012)	0.711 (0.021)
<i>VG</i>	0.553 (0.001)	0.442 (0.005)	0.714 (0.006)	0.716 (0.008)
<i>MI</i>	0.679 (0.015)	0.773 (0.012)	0.796 (0.014)	0.786 (0.007)
<i>SAO</i>	0.541 (0.000)	0.396 (0.001)	0.678 (0.001)	0.666 (0.002)

Table 5: Accuracy on *AmazonReviews*, where a model is trained on five domains and tested on an unseen target.

calibration improves ID calibration and errs on the OOD test set uniformly (w.r.t. the predicted probability). The connection between ID calibration and OOD performance is kept in ERM as well, where naive calibration achieves best ID calibration and OOD performance. Importantly, in both figures we see that miscalibration on a specific bin correlates with more errors on that same bin on the OOD test set.

7.2 Calibration and Model Selection

We test the ability of doing model selection with in-domain calibration metrics on Colored MNIST, as described in Section 6. Using the validation set of two training environments we choose a model with Algorithm 1, according to the best worst-case ECE. Colorings in Colored MNIST are drawn randomly, so we average the results over different instantiations. The average test environment accuracy of the model chosen by our method is 63.1%(± 3.2). It is superior to selection based on the best worst-case validation accuracy over training domains, which chooses a model with 52%(± 0.4) accuracy. The model with overall best test performance has 66.9% accuracy, though of course that requires evaluating on the test set. In Figure 4 we show the test accuracy vs. average worst environment ECE.

8 Conclusion

In this paper we highlight the connection between multi-domain calibration and OOD generalization, arguing that such calibration can be viewed as an invariant representation. We proved in a simplified setting that models calibrated on multiple domains are free of spurious correlations and therefore generalize better. We then proposed multi-domain calibration as a practical and measurable surrogate for the OOD performance of a classifier. We have demonstrated that actively tuning models to achieve multi-domain calibration improves model performance on unseen test domains, and that in-domain calibration on a validation set is a useful criterion for model selection. We hope that this work will spur more research, both empirical and theoretical, on the intriguing link between calibration and OOD generalization.

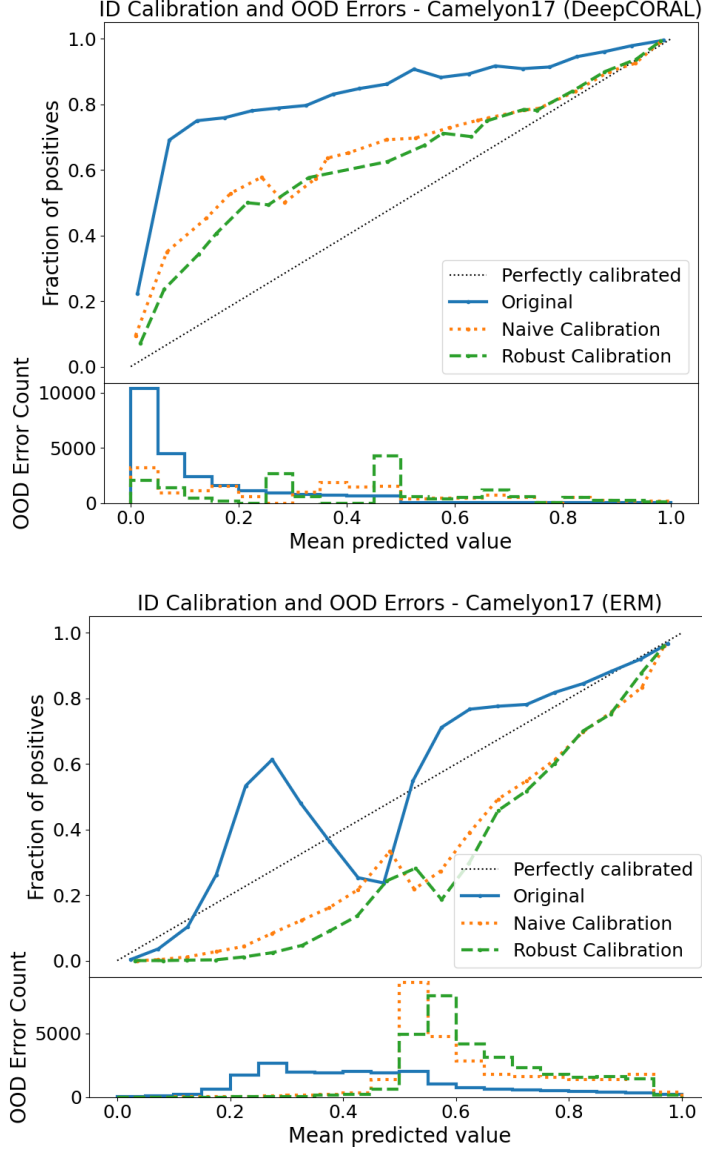


Figure 3: Calibration plots for DeepCORAL (top) and ERM (bottom) on *Camelyon17*. Below each calibration plot: histogram of OOD prediction errors binned by the model’s output values.

Acknowledgments

We wish to thank Ira Shavitt for his helpful comments. This research was partially supported by the Israel Science Foundation (grant No. 1950/19).

References

- [1] M. Arjovsky, L. Bottou, I. Gulrajani, and D. Lopez-Paz. Invariant risk minimization. *arXiv preprint arXiv:1907.02893*, 2019.
- [2] P. Bandi, O. Geessink, Q. Manson, M. Van Dijk, M. Balkenhol, M. Hermsen, B. E. Bejnordi, B. Lee, K. Paeng, A. Zhong, et al. From detection of individual metastases to classification of lymph node status at the patient level: the camelyon17 challenge. *IEEE transactions on medical imaging*, 38(2):550–560, 2018.
- [3] A. Bellot and M. van der Schaar. Generalization and invariances in the presence of unobserved confounding. *arXiv preprint arXiv:2007.10653*, 2020.

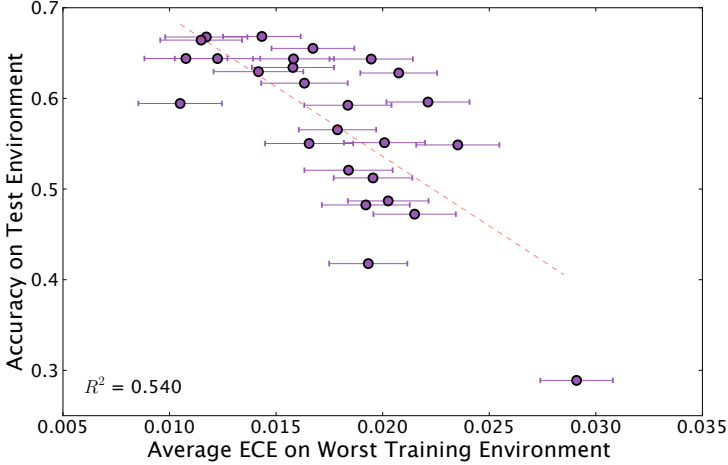


Figure 4: Accuracies on test environment of Colored MNIST for all trained models against their worst-case train ECEs. Dotted line marks a linear fit of the test accuracy from the observed ECE.

- [4] A. Ben-Tal, D. Den Hertog, A. De Waegenaere, B. Melenberg, and G. Rennen. Robust solutions of optimization problems affected by uncertain probabilities. *Management Science*, 59(2):341–357, 2013.
- [5] D. Borkan, L. Dixon, J. Sorensen, N. Thain, and L. Wasserman. Nuanced metrics for measuring unintended bias with real data for text classification. In *Companion proceedings of the 2019 world wide web conference*, pages 491–500, 2019.
- [6] L. Breiman. Random forests. *Machine learning*, 45(1):5–32, 2001.
- [7] G. Christie, N. Fendley, J. Wilson, and R. Mukherjee. Functional map of the world. In *Proceedings of the IEEE Conference on Computer Vision and Pattern Recognition*, pages 6172–6180, 2018.
- [8] M. H. DeGroot and S. E. Fienberg. The comparison and evaluation of forecasters. *Journal of the Royal Statistical Society: Series D (The Statistician)*, 32(1-2):12–22, 1983.
- [9] S. Desai and G. Durrett. Calibration of pre-trained transformers. In *Proceedings of the 2020 Conference on Empirical Methods in Natural Language Processing (EMNLP)*, pages 295–302, 2020.
- [10] J. Devlin, M.-W. Chang, K. Lee, and K. Toutanova. Bert: Pre-training of deep bidirectional transformers for language understanding. In *Proceedings of the 2019 Conference of the North American Chapter of the Association for Computational Linguistics: Human Language Technologies, Volume 1 (Long and Short Papers)*, pages 4171–4186, 2019.
- [11] S. Diamond and S. Boyd. CVXPY: A Python-embedded modeling language for convex optimization. *Journal of Machine Learning Research*, 17(83):1–5, 2016.
- [12] I. Gulrajani and D. Lopez-Paz. In search of lost domain generalization. *arXiv preprint arXiv:2007.01434*, 2020.
- [13] C. Guo, G. Pleiss, Y. Sun, and K. Q. Weinberger. On calibration of modern neural networks. In *International Conference on Machine Learning*, pages 1321–1330. PMLR, 2017.
- [14] R. Guo, P. Zhang, H. Liu, and E. Kiciman. Out-of-distribution prediction with invariant risk minimization: The limitation and an effective fix. *arXiv preprint arXiv:2101.07732*, 2021.
- [15] C. Gupta, A. Podkopaev, and A. Ramdas. Distribution-free binary classification: prediction sets, confidence intervals and calibration. *Advances in Neural Information Processing Systems*, 33, 2020.
- [16] K. He, X. Zhang, S. Ren, and J. Sun. Identity mappings in deep residual networks. In *European conference on computer vision*, pages 630–645. Springer, 2016.
- [17] U. Hébert-Johnson, M. Kim, O. Reingold, and G. Rothblum. Multicalibration: Calibration for the (computationally-identifiable) masses. In *International Conference on Machine Learning*, pages 1939–1948. PMLR, 2018.

[18] C. Heinze-Deml, J. Peters, and N. Meinshausen. Invariant causal prediction for nonlinear models. *Journal of Causal Inference*, 6(2), 2018.

[19] W. Hu, G. Niu, I. Sato, and M. Sugiyama. Does distributionally robust supervised learning give robust classifiers? In *International Conference on Machine Learning*, pages 2029–2037. PMLR, 2018.

[20] G. Huang, Z. Liu, L. Van Der Maaten, and K. Q. Weinberger. Densely connected convolutional networks. In *Proceedings of the IEEE conference on computer vision and pattern recognition*, pages 4700–4708, 2017.

[21] P. Kamath, A. Tangella, D. J. Sutherland, and N. Srebro. Does invariant risk minimization capture invariance? *arXiv preprint arXiv:2101.01134*, 2021.

[22] B. Kim, H. Kim, K. Kim, S. Kim, and J. Kim. Learning not to learn: Training deep neural networks with biased data. In *Proceedings of the IEEE/CVF Conference on Computer Vision and Pattern Recognition*, pages 9012–9020, 2019.

[23] P. W. Koh, S. Sagawa, H. Marklund, S. M. Xie, M. Zhang, A. Balsubramani, W. Hu, M. Yasunaga, R. L. Phillips, S. Beery, et al. Wilds: A benchmark of in-the-wild distribution shifts. *arXiv preprint arXiv:2012.07421*, 2020.

[24] D. Krueger, E. Caballero, J.-H. Jacobsen, A. Zhang, J. Binas, R. L. Priol, and A. Courville. Out-of-distribution generalization via risk extrapolation (rex). *arXiv preprint arXiv:2003.00688*, 2020.

[25] V. Kuleshov, N. Fenner, and S. Ermon. Accurate uncertainties for deep learning using calibrated regression. In *International Conference on Machine Learning*, pages 2796–2804. PMLR, 2018.

[26] A. Kumar, S. Sarawagi, and U. Jain. Trainable calibration measures for neural networks from kernel mean embeddings. In *International Conference on Machine Learning*, pages 2805–2814, 2018.

[27] Y. LeCun. The mnist database of handwritten digits. <http://yann.lecun.com/exdb/mnist/>, 1998.

[28] J. M. Lee. Smooth manifolds. In *Introduction to Smooth Manifolds*, pages 1–31. Springer, 2013.

[29] S. Magliacane, T. van Ommen, T. Claassen, S. Bongers, P. Versteeg, and J. M. Mooij. Domain adaptation by using causal inference to predict invariant conditional distributions. In *Proceedings of the 32nd International Conference on Neural Information Processing Systems*, pages 10869–10879, 2018.

[30] M. P. Naeini, G. Cooper, and M. Hauskrecht. Obtaining well calibrated probabilities using bayesian binning. In *Proceedings of the AAAI Conference on Artificial Intelligence*, volume 29, 2015.

[31] J. Ni, J. Li, and J. McAuley. Justifying recommendations using distantly-labeled reviews and fine-grained aspects. In *Proceedings of the 2019 Conference on Empirical Methods in Natural Language Processing and the 9th International Joint Conference on Natural Language Processing (EMNLP-IJCNLP)*, pages 188–197, 2019.

[32] A. Niculescu-Mizil and R. Caruana. Predicting good probabilities with supervised learning. In *Proceedings of the 22nd international conference on Machine learning*, pages 625–632, 2005.

[33] J. Nixon, M. W. Dusenberry, L. Zhang, G. Jerfel, and D. Tran. Measuring calibration in deep learning. In *IEEE Conference on Computer Vision and Pattern Recognition Workshops, CVPR Workshops 2019, Long Beach, CA, USA, June 16-20, 2019*, pages 38–41. Computer Vision Foundation / IEEE, 2019.

[34] N. Oved, A. Feder, and R. Reichart. Predicting in-game actions from interviews of nba players. *Computational Linguistics*, 46(3):667–712, 2020.

[35] J. Peters, P. Bühlmann, and N. Meinshausen. Causal inference by using invariant prediction: identification and confidence intervals. *Journal of the Royal Statistical Society. Series B (Statistical Methodology)*, pages 947–1012, 2016.

[36] J. Platt et al. Probabilistic outputs for support vector machines and comparisons to regularized likelihood methods. *Advances in large margin classifiers*, 10(3):61–74, 1999.

[37] G. Pleiss, M. Raghavan, F. Wu, J. Kleinberg, and K. Q. Weinberger. On fairness and calibration. *arXiv preprint arXiv:1709.02012*, 2017.

- [38] E. Rosenfeld, P. Ravikumar, and A. Risteski. The risks of invariant risk minimization. *arXiv preprint arXiv:2010.05761*, 2020.
- [39] D. Rothenhäusler, N. Meinshausen, P. Bühlmann, and J. Peters. Anchor regression: heterogeneous data meets causality. *arXiv preprint arXiv:1801.06229*, 2018.
- [40] S. Sagawa, P. W. Koh, T. B. Hashimoto, and P. Liang. Distributionally robust neural networks for group shifts: On the importance of regularization for worst-case generalization. *arXiv preprint arXiv:1911.08731*, 2019.
- [41] B. Schölkopf, D. Janzing, J. Peters, E. Sgouritsa, K. Zhang, and J. Mooij. On causal and anticausal learning. *arXiv preprint arXiv:1206.6471*, 2012.
- [42] A. W. Senior, R. Evans, J. Jumper, J. Kirkpatrick, L. Sifre, T. Green, C. Qin, A. Zídek, A. W. R. Nelson, A. Bridgland, H. Penedones, S. Petersen, K. Simonyan, S. Crossan, P. Kohli, D. T. Jones, D. Silver, K. Kavukcuoglu, and D. Hassabis. Improved protein structure prediction using potentials from deep learning. *Nat.*, 577(7792):706–710, 2020.
- [43] E. Shabat, L. Cohen, and Y. Mansour. Sample complexity of uniform convergence for multicalibration. *arXiv preprint arXiv:2005.01757*, 2020.
- [44] A. Subbaswamy, P. Schulam, and S. Saria. Preventing failures due to dataset shift: Learning predictive models that transport. In *The 22nd International Conference on Artificial Intelligence and Statistics*, pages 3118–3127. PMLR, 2019.
- [45] B. Sun and K. Saenko. Deep coral: Correlation alignment for deep domain adaptation. In *European conference on computer vision*, pages 443–450. Springer, 2016.
- [46] A. Vaswani, N. Shazeer, N. Parmar, J. Uszkoreit, L. Jones, A. N. Gomez, Ł. Kaiser, and I. Polosukhin. Attention is all you need. In *Advances in neural information processing systems*, pages 5998–6008, 2017.
- [47] X. Wang, M. Long, J. Wang, and M. I. Jordan. Transferable calibration with lower bias and variance in domain adaptation. *arXiv preprint arXiv:2007.08259*, 2020.
- [48] C. Yeh, A. Perez, A. Driscoll, G. Azzari, Z. Tang, D. Lobell, S. Ermon, and M. Burke. Using publicly available satellite imagery and deep learning to understand economic well-being in africa. *Nature communications*, 11(1):1–11, 2020.
- [49] B. Zadrozny and C. Elkan. Obtaining calibrated probability estimates from decision trees and naive bayesian classifiers. In C. E. Brodley and A. P. Danyluk, editors, *Proceedings of the Eighteenth International Conference on Machine Learning (ICML 2001), Williams College, Williamstown, MA, USA, June 28 - July 1, 2001*, pages 609–616. Morgan Kaufmann, 2001.

A Proofs for Theoretical Claims

We begin by supplementing the definition of multiple domain calibration, extending it for the case of regression, then we provide proofs of the theorems in the paper.

A.1 Definition of Calibration

Recall our definition of a calibrated classifier for binary tasks.

Definition S1 *Let $f : \mathcal{X} \rightarrow [0, 1]$ and $P[X, Y]$ be a joint distribution over the features and label. Then $f(\mathbf{x})$ is calibrated w.r.t to P if for all $\alpha \in [0, 1]$ in the range of f :*

$$\mathbb{E}_P[Y \mid f(X) = \alpha] = \alpha.$$

In the multiple environments setting, $f(\mathbf{x})$ is calibrated on E_{train} if for all $e_i \in E_{\text{train}}$ and α in the range of f restricted to e_i :

$$\mathbb{E}[Y \mid f(X) = \alpha, E = e_i] = \alpha.$$

For regression tasks, one may consider a function that outputs a full CDF on Y and define a calibrated classifier as one where all quantiles of the CDF match the true quantiles of Y as the number of examples approached infinity. This leads to the definition in [25], and one may follow this to analyze more general cases than the scenario we will consider in this work.

Since in this section we consider Gaussian distributions and linear regressors, a definition based on the first two moments of the distribution (instead of all quantiles of a CDF) will suffice. Hence we will be working the following definition:

Definition S2 *Let $f : \mathcal{X} \rightarrow \mathbb{R}^2$ and $P[X, Y]$ a joint distribution over the features and label. Then $f(\mathbf{x})$ is calibrated w.r.t to P if for all $(\alpha, \beta) \in \mathbb{R}^2$ in the range of f :*

$$\mathbb{E}[Y \mid f(X)_1 = \alpha] = \alpha, \mathbb{E}[Y^2 \mid f(X)_2 = \beta] = \beta.$$

In the multiple environments setting, $f(\mathbf{x})$ is calibrated on E_{train} if for all $e_i \in E_{\text{train}}$ and (α, β) in the range of f restricted to e_i :

$$\mathbb{E}[Y \mid f(X) = (\alpha, \beta), E = e_i] = \alpha, \mathbb{E}[Y^2 \mid f(X) = (\alpha, \beta), E = e_i] = \beta. \quad (7)$$

Equipped with these definitions, we can now turn to the proofs of the theorems in the paper.

A.2 Classification with Invariant Features

We first consider the classification task from the main paper, where the data generating process is described in Figure S1. Recall that we are considering linear classifiers of the form $f(\mathbf{x}; \mathbf{w}, b) = \sigma(\mathbf{w}^\top \mathbf{x} + b)$. Our environments here are defined by the parameters of the multivariate Gaussian distributions that generate the spurious features $\{\mu_i, \Sigma_i\}_{i=1}^k$. As a first step we will derive the algebraic form of the constraints that calibration imposes on \mathbf{w} and the parameters defining the environments.

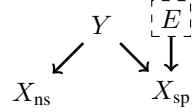


Figure S1: Diagram for data generating process in the invariant features scenario.

Lemma S1 *Assume we have k environments with means and covariance matrices for environmental features $\mu_i \in \mathbb{R}^{d_e}$, $\Sigma_i \in \mathbb{S}_{++}^{d_e}$, $i \in [k]$ and a common covariance matrix $\Sigma_{ns} \in \mathbb{S}_{++}^{d_{ns}}$ for invariant features, where data is generated according to:*

$$y = \begin{cases} 1 & \text{w.p } \eta \\ -1 & \text{otherwise,} \end{cases} \quad \begin{aligned} \mathbf{x}_{ns} \mid Y = y &\sim \mathcal{N}(y\mu_{ns}, \Sigma_{ns}), \\ \mathbf{x}_{sp} \mid Y = y &\sim \mathcal{N}(y\mu_i, \Sigma_i), \end{aligned}$$

and $\mathbf{x}_{ns}, \mathbf{x}_{sp}$ are drawn independently. Let $\sigma : \mathbb{R} \rightarrow (0, 1)$ be an invertible function and define the classifier:

$$f(\mathbf{x}; \mathbf{w}, b) = \sigma(\mathbf{w}^\top \mathbf{x} - b).$$

Decompose the weights $\mathbf{w} = [\mathbf{w}_{ns}, \mathbf{w}_{sp}]$ to the coefficients of the invariant and spurious features accordingly. Then if the classifier is calibrated on all environments, it holds that either $\mathbf{w} = \mathbf{0}$ or there exists $t \neq 0$ such that:

$$\frac{\mathbf{w}_{ns}^\top \mu_{ns} + \mathbf{w}_{sp}^\top \mu_i}{\mathbf{w}_{ns}^\top \Sigma_{ns} \mathbf{w}_{ns} + \mathbf{w}_{sp}^\top \Sigma_i \mathbf{w}_{sp}} = t \quad \forall i \in [k]. \quad (8)$$

Proof Let $i \in [k]$, the joint distribution of features in the environment is Gaussian with mean $\hat{\mu}_i = [\mu_{ns}, \mu_i]$, covariance $\hat{\Sigma}_i = \begin{bmatrix} \Sigma_{ns} & 0 \\ 0 & \Sigma_i \end{bmatrix}$. Hence the output of the affine function corresponding to the classifier is a random variable with probability density function:

$$P[\sigma^{-1}(f(X)) = \alpha \mid Y = y, E = e_i] = (2\pi \mathbf{w}^\top \hat{\Sigma}_i \mathbf{w})^{-\frac{1}{2}} \exp\left(\frac{(\alpha - y\mathbf{w}^\top \hat{\mu}_i + b)^2}{2\mathbf{w}^\top \hat{\Sigma}_i \mathbf{w}}\right).$$

Hence the conditional probability of Y is given by:

$$P[Y = 1 \mid \sigma^{-1}(f(X)) = \alpha, E = e_i] = \frac{\eta \exp\left(\frac{(\alpha - \mathbf{w}^\top \hat{\mu}_i + b)^2}{2\mathbf{w}^\top \hat{\Sigma}_i \mathbf{w}}\right)}{\eta \exp\left(\frac{(\alpha - \mathbf{w}^\top \hat{\mu}_i + b)^2}{2\mathbf{w}^\top \hat{\Sigma}_i \mathbf{w}}\right) + (1 - \eta) \exp\left(\frac{(\alpha + \mathbf{w}^\top \hat{\mu}_i + b)^2}{2\mathbf{w}^\top \hat{\Sigma}_i \mathbf{w}}\right)}.$$

Note that unless $\mathbf{w} = \mathbf{0}$ (which results in a calibrated classifier that satisfies Equation (8)), the variance of $\sigma^{-1}(f(X))$ is strictly positive since $\hat{\Sigma}_i \succ 0$, so above conditional probabilities are well-defined. Now it is easy to see that if the classifier is calibrated across environments, we need to have equality in the log-odds ratio for each i, j and all $\alpha \in \mathbb{R}$:

$$\frac{(\alpha - \mathbf{w}^\top \hat{\mu}_i + b)^2}{2\mathbf{w}^\top \hat{\Sigma}_i \mathbf{w}} - \frac{(\alpha + \mathbf{w}^\top \hat{\mu}_i + b)^2}{2\mathbf{w}^\top \hat{\Sigma}_i \mathbf{w}} = \frac{(\alpha - \mathbf{w}^\top \hat{\mu}_j + b)^2}{2\mathbf{w}^\top \hat{\Sigma}_j \mathbf{w}} - \frac{(\alpha + \mathbf{w}^\top \hat{\mu}_j + b)^2}{2\mathbf{w}^\top \hat{\Sigma}_j \mathbf{w}} \quad \forall \alpha \in \mathbb{R}.$$

After dropping all the terms that cancel out in the subtractions we arrive at:

$$\frac{\mathbf{w}^\top \hat{\mu}_i}{\mathbf{w}^\top \hat{\Sigma}_i \mathbf{w}} = \frac{\mathbf{w}^\top \hat{\mu}_j}{\mathbf{w}^\top \hat{\Sigma}_j \mathbf{w}}.$$

This may also be written as a system of equations with an additional scalar variable $t \in \mathbb{R}$:

$$\frac{\mathbf{w}^\top \hat{\mu}_i}{\mathbf{w}^\top \hat{\Sigma}_i \mathbf{w}} = t \quad \forall i \in [k].$$

Now because we assumed $\Sigma_i \succ 0$ for all environments, for any solution to the above system with $t = 0$, we must have:

$$\mathbf{w}^\top \hat{\mu}_i = 0 \quad \forall i \in [k].$$

Furthermore we will have for any $\alpha \in \mathbb{R}$:

$$P[Y = 1 \mid \sigma^{-1}(f(X)) = \alpha, E = e_i] = \eta.$$

Since we assume f is calibrated and the right hand side needs to equal α , this is only possible if $f(\mathbf{x}; \mathbf{w}, b)$ is a constant function. Again, because $\Sigma_i \succ 0$, this is only possible if $\mathbf{w} = \mathbf{0}$. Hence we conclude with our desired result, as can be seen by decomposing \mathbf{w} to the parts corresponding to invariant and spurious features. \blacksquare

We now give a result for the special case where the covariance matrices of the spurious features satisfy $\Sigma_i = \sigma_i^2 \mathbf{I}$, considered in [38]. The nice correspondence here is that we will see that calibration demands one more environment than IRM to discard all spurious features. This matches the intuition that each environment reduces a degree of freedom from the set of invariant classifiers, while risk minimization reduces one more degree of freedom.

Lemma S2 *Assume we have $k \geq d_{sp} + 2$ environments and define $M(\{\mu_i, \sigma_i\}_{i=1}^k) \in \mathbb{R}^{k \times d_e + 2}$:*

$$M(\{\mu_i, \sigma_i\}_{i=1}^k) = \begin{bmatrix} \mu_1^\top & \sigma_1^2 & 1 \\ & \vdots & \\ \mu_k^\top & \sigma_k^2 & 1 \end{bmatrix}.$$

If the matrix has full rank, then for any invariant predictor the linear coefficients on spurious features are zero.

Proof According to Lemma S1, writing down the conditional probability $P[Y \mid \sigma^{-1}(f(\mathbf{x})), E = e]$ and demanding calibration results in the constraint that either $\mathbf{w} = \mathbf{0}$, and then the linear coefficients on spurious features are indeed 0; or that for some $t \neq 0$:

$$\frac{\mathbf{w}_{ns}^\top \mu_{ns} + \mathbf{w}_{sp}^\top \mu_i}{\mathbf{w}_{ns}^\top \Sigma_{ns} \mathbf{w}_{ns} + \sigma_i^2 \|\mathbf{w}_{sp}\|_2^2} = t \quad \forall i \in [k].$$

Without loss of generality we can phrase these constraints as:

$$\frac{\mathbf{w}_{ns}^\top \mu_{ns} + \mathbf{w}_{sp}^\top \mu_i}{\mathbf{w}_{ns}^\top \Sigma_{ns} \mathbf{w}_{ns} + \sigma_i^2 \|\mathbf{w}_{sp}\|_2^2} = 1 \quad \forall i \in [k].$$

This is true since if \mathbf{w} is a solution to this system of equations where the right hand side is some $t \in \mathbb{R}$ then $t\mathbf{w}$ is a solution to the system where t is replaced by 1. Rewrite the constraints again to isolate the parts depending on \mathbf{w}_{sp} :

$$\sigma_i^2 \|\mathbf{w}_{sp}\|_2^2 - \mu_i^\top \mathbf{w}_{sp} = \mathbf{w}_{ns}^\top \Sigma_{ns} \mathbf{w}_{ns} - \mathbf{w}_{ns}^\top \mu_{ns} \quad \forall i \in [k].$$

To find whether this system has a solution where \mathbf{w}_{sp} is non-zero we can replace the right hand side with a scalar variable $t \in \mathbb{R}$, and ask whether the following system has a non-zero solution:

$$\sigma_i^2 \|\mathbf{w}_{sp}\|_2^2 - \mu_i^\top \mathbf{w}_{sp} = t \quad \forall i \in [k].$$

For the above equations to have a non-zero solution, the following linear system must also have such a solution:

$$M(\{\mu_i, \sigma_i\}_{i=1}^k) \mathbf{x} = \mathbf{0}.$$

But from our non-degeneracy condition, such a solution does not exist. \blacksquare

Next we generalize the above to prove the result from the main paper, namely when the matrices $\{\Sigma_i\}_{i=1}^k$ are not diagonal. For this purpose we introduce a definition of general position for environments, similar to the one given in [1].

Definition S3 *Given $k > 2d_{sp}$ environments with mean parameters $\{\Sigma_i, \mu_i\}_{i=1}^k$, we say they are in general position if for all non-zero $\mathbf{x} \in \mathbb{R}_{sp}^d$:*

$$\dim \left(\text{span} \left\{ \begin{bmatrix} \Sigma_i \mathbf{x} + \mu_i \\ 1 \end{bmatrix} \right\}_{i \in [k]} \right) = d_e + 1.$$

Equipped with this notion of general position, we now need to show that if it holds then the only predictors that satisfy the conditions of Lemma S1 are those with $\mathbf{w}_{sp} = \mathbf{0}$. Another claim we will need to prove is that the subset of environments which do not lie in general position have measure zero in the set of all possible environment settings. Hence generic environments are expected to lie in general position. This argument will follow the lines of the one given in [1], adapted to our case with the fixed coordinate 1 added in the above definition.

Theorem 1 *Under the setting of Lemma S1, if the environments lie in general position then all classifiers that are calibrated across environments satisfy $\mathbf{w}_{sp} = \mathbf{0}$.*

Proof According to Lemma S1, if the predictor is calibrated then Equation (8) must hold. Following the same arguments laid out in the proof at the main paper, we get that \mathbf{w}_{sp} needs to be a solution for the following system of equations:

$$\mathbf{w}_{sp}^\top \Sigma_i \mathbf{w}_{sp} - \mu_i^\top \mathbf{w}_{sp} - t = 0 \quad \forall i \in [k]. \quad (9)$$

Now, let $\mathbf{w}_{sp} \in \mathbb{R}^{d_{sp}}$ be a non-zero vector and let us define the $k \times d_e + 1$ matrix:

$$M(\{\mu_i, \Sigma_i\}_{i=1}^k, \mathbf{w}_{sp}) = \begin{bmatrix} \mathbf{w}_{sp}^\top \Sigma_1 - \mu_1^\top & 1 \\ \vdots & \\ \mathbf{w}_{sp}^\top \Sigma_k - \mu_k^\top & 1 \end{bmatrix}$$

If the environments are in general position, the above matrix has full rank for any non-zero \mathbf{w}_{sp} . Similarly to the proof of Lemma S2, if Equation (9) has a non-zero solution then the following system must also have a solution:

$$M(\{\mu_i, \Sigma_i\}_{i=1}^k, \mathbf{w}_{sp}) \mathbf{x} = \mathbf{0}.$$

Which is of course impossible due to $M(\{\mu_i, \Sigma_i\}_{i=1}^k, \mathbf{w}_{sp})$ having full rank. \blacksquare

We conclude with the statement about the measure of sets of environments which do not lie in general position, this will follow the lines of [1].

Lemma S3 Let $k > 2d_{sp}$ and $\{\mu_i\}_{i=1}^k$ be arbitrary fixed vectors, then the set of matrices $\{\Sigma_i\}_{i=1}^k \in (\mathbb{S}_{++}^{d_{sp}})^k$ for which $\{\Sigma_i, \mu_i\}_{i=1}^k$ do not lie in general position has measure zero within the set $(\mathbb{S}_{++}^{d_{sp}})^k$.

Proof We assume $k > 2d_{sp}$ and denote by $LR(k, d_{sp}, r)$ the matrices of dimensions $k \times d_{sp}$ and rank r . Also for any d denote by $\mathbf{1}_d$ the vector in \mathbb{R}^d where all entries equal 1. Define $\mathbf{M}_*^1(k, d_{sp})$ as the set of $k \times d_{sp}$ matrices of full column-rank whose columns span the vector of ones $\mathbf{1}_k$:

$$\mathbf{M}_*^1(k, d_{sp}) = \{A \in LR(k, d_{sp}, d_{sp}) \mid \mathbf{1}_k \in \text{colsp}(A)\}.$$

Let $\{\Sigma_i\}_{i=1}^k \in (\mathbb{S}_{++}^{d_{sp}})^k$ and define $\mathbf{W} \subseteq \mathbb{R}^{k \times d_{sp}}$ as the image of the mapping $G : \mathbb{R}^{d_{sp}} \setminus \{0\} \rightarrow \mathbb{R}^{k \times d_{sp}}$:

$$(G(\mathbf{x}))_{i,l} = (\Sigma_i \mathbf{x} - \mu_i)_l$$

By the definition of general position given in the paper, the environments defined by $\{\Sigma_i, \mu_i\}_{i=1}^k$ lie in general position if \mathbf{W} does not intersect $LR(k, d_{sp}, r)$ for all $r < d_{sp}$ and $\mathbf{M}_*^1(k, d_{sp})$. We would like to show that this happens for all but a measure zero of $(\mathbb{S}_{++}^{d_{sp}})^k$.

Due to the exact same arguments in Thoerem 10 of [1], we have that \mathbf{W} is transversal to any submanifold of $\mathbb{R}^{k \times d_{sp}}$ and also does not intersect $LR(k, d_{sp}, r)$ where $r < d_{sp}$, for all $\{\Sigma_i\}_{i=1}^k$ but a measure zero of $(\mathbb{S}_{++}^{d_{sp}})^k$.

It is left to show that it also does not intersect $\mathbf{M}_*^1(k, d_{sp})$ for all but a measure zero of $(\mathbb{S}_{++}^{d_{sp}})^k$. Because $\mathbf{M}_*^1(k, d_{sp})$ is a submanifold of $\mathbb{R}^{k \times d_{sp}}$, it intersects transversally with \mathbf{W} for generic $\{\Sigma_i\}_{i=1}^k$. Then by transversality they cannot intersect if $\dim(\mathbf{W}) + \dim(\mathbf{M}_*^1(k, d_{sp})) - \dim(\mathbb{R}^{k \times d_{sp}}) < 0$. We will claim that $\dim(\mathbf{M}_*^1(k, d_{sp})) = k(d_{sp} - 1) + d_{sp}$ and then since $k > 2d_{sp}$ we may obtain:

$$\begin{aligned} \dim(\mathbf{W}) + \dim(\mathbf{M}_*^1(k, d_{sp})) - \dim(\mathbb{R}^{k \times d_{sp}}) &\leq d_{sp} + k(d_{sp} - 1) + d_{sp} - kd_{sp} \\ &= 2d_{sp} - k \\ &< 0. \end{aligned}$$

The negativity of the dimension implies that if \mathbf{W} and $\mathbf{M}_*^1(k, d_{sp})$ are transversal then they do not intersect, and we may conclude our desired result that the environments lie in general position for all but a measure zero of $(\mathbb{S}_{++}^{d_{sp}})^k$.

To show that $\dim(\mathbf{M}_*^1(k, d_{sp})) = k(d_{sp} - 1) + d_{sp}$, consider a matrix $A \in \mathbf{M}_*^1(k, d_{sp})$. Since it has full rank, it has a $d_{sp} \times d_{sp}$ minor that is invertible. Assume this minor is just the first d_{sp} rows of A , otherwise there is a linear isomorphism that transforms it into such a matrix and the arguments that follow still apply (see [28], Example 5.30; our proof follows a similar line of reasoning). Now write A as a block matrix using $B \in \mathbb{R}^{d_{sp} \times d_{sp}}$, $C \in \mathbb{R}^{(k-d_{sp}) \times d_{sp}}$:

$$\begin{bmatrix} B \\ C \end{bmatrix}.$$

Denoting by \mathbf{U} the set of $k \times d_{sp}$ matrices whose first d_{sp} rows are invertible, we consider the mapping $F : \mathbf{U} \rightarrow \mathbb{R}^{k-d_{sp}}$:

$$F(A) = \mathbf{1}_{k-d_{sp}} - CB^{-1}\mathbf{1}_{d_{sp}}.$$

Clearly $F^{-1}(\mathbf{0}) = \mathbf{M}_*^1(k, d_{sp})$ and F is smooth. We will show that it is a submersion by observing that its differential $DF(U)$ is surjective for each $U \in \mathbf{U}$. To this end, for a given $U = \begin{bmatrix} B \\ C \end{bmatrix}$ and any $X \in \mathbb{R}^{(k-d_{sp}) \times d_{sp}}$ define a curve $\gamma : (-\epsilon, \epsilon) \rightarrow \mathbf{U}$ by:

$$\gamma(t) = \begin{bmatrix} B \\ C + \gamma X \end{bmatrix}.$$

We have that:

$$(F \circ \gamma)'(t) = \frac{d}{dt}|_{t=0}(\mathbf{1}_{k-d_{sp}} - (C + tX)B^{-1}\mathbf{1}_{d_{sp}}) = XB^{-1}\mathbf{1}_{d_{sp}}.$$

Since $B^{-1}\mathbf{1}_{d_{sp}}$ is not the zero vector, and $X \in \mathbb{R}^{(k-d_{sp}) \times d_{sp}}$ where $k - d_{sp} > d_{sp}$, then it is clear that the above mapping is surjective. Note that the derivatives along the curve are just a subset of the range of $DF(U)$, hence $DF(U)$ is also surjective at each point $U \in \mathbf{U}$. It follows from the submersion theorem that $\dim(\mathbf{M}_*^1(k, d_{sp})) = kd_{sp} - (k - d_{sp}) = k(d_{sp} - 1) + d_{sp}$ as desired for our result to hold. \blacksquare

A.3 Regression Under Covariate Shift and Spurious Features

We now move on to the second scenario presented in the paper where the mechanism $P(Y | X)$ is invariant and the diagram depicting the data generating process is given in Figure S2. Here for each environment $i \in [k]$ we will have:

$$\begin{aligned} X_c &\sim \mathcal{N}(\mu_i^c, \Sigma_i^c) \\ Y &= \mathbf{w}_c^{*\top} \mathbf{x}_c + \xi, \quad \xi \sim \mathcal{N}(0, \sigma_y^2) \\ X_{sp} &= y\mu_i + \eta, \quad \eta \sim \mathcal{N}(\mathbf{0}, \Sigma_i). \end{aligned}$$

We consider a regressor $f : \mathcal{X} \rightarrow \mathbb{R}^2$, where the estimate of the mean is linear, i.e. $[f(\mathbf{x}; \mathbf{w})]_1 = \mathbf{w}^\top \mathbf{x}$, and the estimate of the variance is constant $[f(\mathbf{x}; \mathbf{w})]_2 = c$.⁴ We decompose the weights \mathbf{w} into their parts corresponding to causal and spurious features $[\mathbf{w}_c, \mathbf{w}_{sp}]$. Then our result regarding calibration and generalization to \mathcal{E} is given below.

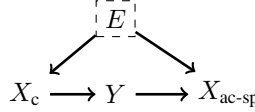


Figure S2: Diagram for data generating process in the covariate shift scenario.

Theorem 2 Denote the dimensions of X_c, X_{sp} by d_c, d_{sp} accordingly. Assume we have k environments with parameters $\{\mu_i^c, \mu_i, \Sigma_i^c, \Sigma_i\}_{i=1}^k$. For any matrix A denote its i -th row by A^i , and define the matrices $M(\{\mu_i^c, \mu_i\}_{i=1}^k) \in \mathbb{R}^{k \times d_c + d_{sp} + 1}$ and $M_2(\{\mu_i^c, \Sigma_i^c\}_{i=1}^k, \sigma_y^2, \mathbf{w}_c^*) \in \mathbb{R}^{k \times d_c + 2}$ whose rows are given by:

$$\begin{aligned} M(\{\mu_i^c, \mu_i\}_{i=1}^k) &= \begin{bmatrix} \mu_1^{c\top} & (\mathbf{w}_c^{*\top} \mu_1^c) \mu_1^\top & 1 \\ \vdots & \vdots & \vdots \\ \mu_k^{c\top} & (\mathbf{w}_c^{*\top} \mu_k^c) \mu_k^\top & 1 \end{bmatrix}, \\ M_2(\{\mu_i^c, \Sigma_i^c\}_{i=1}^k, \sigma_y^2, \mathbf{w}_c^*) &= \begin{bmatrix} \mathbf{w}_c^{*\top} \Sigma_1^c + \left(\frac{\mathbf{w}_c^{*\top} \Sigma_1^c \mathbf{w}_c^* + \sigma_y^2}{\mathbf{w}_c^{*\top} \mu_1^c} \right) \mu_1^{c\top} & \frac{\mathbf{w}_c^{*\top} \Sigma_1^c \mathbf{w}_c^*}{\mathbf{w}_c^{*\top} \mu_1^c} & 1 \\ \vdots & \vdots & \vdots \\ \mathbf{w}_c^{*\top} \Sigma_k^c + \left(\frac{\mathbf{w}_c^{*\top} \Sigma_k^c \mathbf{w}_c^* + \sigma_y^2}{\mathbf{w}_c^{*\top} \mu_k^c} \right) \mu_k^{c\top} & \frac{\mathbf{w}_c^{*\top} \Sigma_k^c \mathbf{w}_c^*}{\mathbf{w}_c^{*\top} \mu_k^c} & 1 \end{bmatrix}. \end{aligned}$$

Let $f(\mathbf{x}; \mathbf{w})$ be a calibrated regressor, assume $\mathbf{w}_c^{*\top} \mu_i^c \neq 0$ for all $i \in [k]$ and that there exists $i, j \in [k]$ such that $\mathbb{E}[Y | E = e_i] \neq \mathbb{E}[Y | E = e_j]$. Furthermore assume that one of the following conditions hold:

- $k > \max\{d_c + 2, d_{sp}\}$, $M_2(\{\mu_i^c, \Sigma_i^c\}_{i=1}^k, \sigma_y^2, \mathbf{w}_c^*)$ has full rank and the means of spurious features $\{\mu_i\}_{i=1}^k$ span $\mathbb{R}^{d_{sp}}$.
- $k > d_c + d_{sp} + 1$ and $M(\{\mu_i^c, \mu_i\}_{i=1}^k)$ has full rank.

⁴Limiting the variance estimate to a constant does not make a difference for the purpose of our proof. The proof does not rely on the correctness of the variance estimate as imposed by Equation (7), but only on the variances being equal across environments when conditioned on $f(\mathbf{x})$. In other words it relies on the correctness of the mean estimate, and the distribution of Y conditioned on $f(X)$ being the same across environments.

then the weights of f must be $\mathbf{w} = [\mathbf{w}_c^*, \mathbf{0}]$.

It is rather clear that rank-deficiency of M_2 would impose some highly non-trivial conditions on the relationships between μ_i^c , $\mathbf{w}_c^{*\top} \Sigma_i^c$ and the conditions given above are satisfied for all settings of environments other than a measure zero under any absolutely continuous measure on the parameters $\mathbf{w}_c^*, \{\mu_i^c, \Sigma_i^c\}_{i=1}^k$. The proof proceeds by writing the conditional distribution of Y on $f(X)$, and showing that the conditions in the theorem are the direct result of the calibration constraints.

Proof Since X_c, X_{sp}, Y are jointly Gaussian, we can write their distribution at environment $i \in [k]$ as:

$$\begin{bmatrix} X_c \\ X_{sp} \\ Y \end{bmatrix} \sim \mathcal{N} \left(\begin{bmatrix} \mu_i^c \\ (\mathbf{w}_c^{*\top} \mu_i^c) \mu_i \\ \mathbf{w}_c^{*\top} \mu_i^c \end{bmatrix}, \begin{bmatrix} \Sigma_i^c & \Sigma_i^c \mathbf{w}_c^* \mu_i^c & \Sigma_i^c \mathbf{w}_c^* \\ \mu_i \mathbf{w}_c^{*\top} \Sigma_i^c & \left(\mathbf{w}_c^{*\top} \Sigma_i^c \mathbf{w}_c^* + \sigma_y^2 \right) \mu_i \mu_i^{\top} + \Sigma_i & \left(\mathbf{w}_c^{*\top} \Sigma_i^c \mathbf{w}_c^* + \sigma_y^2 \right) \mu_i \\ \mathbf{w}_c^{*\top} \Sigma_i^c & (\mathbf{w}_c^{*\top} \Sigma_i^c \mathbf{w}_c^* + \sigma_y^2) \mu_i^{\top} & \mathbf{w}_c^{*\top} \Sigma_i^c \mathbf{w}_c^* + \sigma_y^2 \end{bmatrix} \right).$$

The predictions $\mathbf{w}^{\top} X$ are then also normally distributed, and jointly with Y this can be written as:

$$\begin{bmatrix} \mathbf{w}^{\top} X \\ Y \end{bmatrix} \sim \mathcal{N} \left(\begin{bmatrix} \mathbf{w}_c^{\top} \mu_i^c + (\mathbf{w}_{sp}^{\top} \mu_i) (\mathbf{w}_c^{*\top} \mu_i^c) \\ \mathbf{w}_c^{*\top} \mu_i^c \end{bmatrix}, \begin{bmatrix} \sigma_{f,i}^2 & \sigma_{f,y,i} \\ \sigma_{f,y,i} & \sigma_{y,i}^2 \end{bmatrix} \right),$$

where we defined the items of the covariance matrix:

$$\begin{aligned} \sigma_{f,i}^2 &= \mathbf{w}_c^{\top} \Sigma_i^c \mathbf{w}_c + 2(\mathbf{w}_c^{\top} \Sigma_i^c \mathbf{w}_c^*) (\mu_i^{\top} \mathbf{w}_{sp}) + \mathbf{w}_{sp}^{\top} \left(\mu_i \mu_i^{\top} (\mathbf{w}_c^{*\top} \Sigma_i^c \mathbf{w}_c^* + \sigma_y^2) + \Sigma_i \right) \mathbf{w}_{sp}, \\ \sigma_{f,y,i} &= \mathbf{w}_c^{*\top} \Sigma_i^c \mathbf{w}_c + (\mathbf{w}_c^{*\top} \Sigma_i^c \mathbf{w}_c^* + \sigma_y^2) \mu_i^{\top} \mathbf{w}_{sp}, \\ \sigma_{y,i}^2 &= \mathbf{w}_c^{*\top} \Sigma_i^c \mathbf{w}_c^* + \sigma_y^2. \end{aligned}$$

Now we can write the mean of the conditional distribution of Y on $f(X)_1 = \alpha$ as:

$$\mathbb{E}[Y | f(X)_1 = \alpha, E = e_i] = \mathbf{w}_c^{*\top} \mu_i^c + \frac{\sigma_{f,y,i}}{\sigma_{f,i}^2} (\alpha - \mathbf{w}_c^{\top} \mu_i^c - (\mathbf{w}_{sp}^{\top} \mu_i) (\mathbf{w}_c^{*\top} \mu_i^c)).$$

For each environment $i \in [k]$, the above is a linear function of α . Demanding $f(X)$ to be calibrated on all environments then imposes both the slopes and intercepts to be equal across environments. Writing this for the slope, we obtain that there must exist $t \in \mathbb{R}$ such that:

$$\frac{\sigma_{f,y,i}}{\sigma_{f,i}^2} = t \quad \forall i \in [k]. \quad (10)$$

We note that $t \neq 0$ since if it is zero then we have that $\mathbb{E}[Y | f(X)_1 = \alpha, E = i]$ does not depend on α , where calibration demands that it equals α . This can only happen if $\mathbf{w}_c = \mathbf{0}$, otherwise the range of $f(\mathbf{x})$ is \mathbb{R} because we assumed in the definition of the environments that $\Sigma_c^i \succ 0$. Furthermore, $\mathbf{w}_c = \mathbf{0}$ cannot be calibrated if $\mathbb{E}[Y | E = e_i]$ is not constant across environments; which is also part of the non-degeneracy constraints we required. Next we demand the equality of the intercepts across environments. Taking these equations and replacing Equation (10) into each of them, we get:

$$\mathbf{w}_c^{*\top} \mu_i^c - t \left(\mathbf{w}_c^{\top} \mu_i^c + (\mathbf{w}_{sp}^{\top} \mu_i) (\mathbf{w}_c^{*\top} \mu_i^c) \right) = \mathbf{w}_c^{*\top} \mu_j^c - t \left(\mathbf{w}_c^{\top} \mu_j^c + (\mathbf{w}_{sp}^{\top} \mu_j) (\mathbf{w}_c^{*\top} \mu_j^c) \right) \quad \forall i, j \in [k].$$

Dividing both sides by t and defining $\bar{\mathbf{w}}_c = \frac{\mathbf{w}_c^*}{t} - \mathbf{w}_c$, we can introduce another variable $t_2 \in \mathbb{R}$ and write this as a linear system of equations in variables $\mathbf{w}_{sp}, \bar{\mathbf{w}}_c, t_2$:

$$\bar{\mathbf{w}}_c^{\top} \mu_i^c - \mathbf{w}_{sp}^{\top} \mu_i (\mathbf{w}_c^{*\top} \mu_i^c) + t_2 = 0 \quad \forall i \in [k]. \quad (11)$$

We see that given $d_c + d_{sp} + 1$ environments, then with mild conditions on their non-degeneracy (i.e. the vectors containing the environment means and an extra entry of 1 span $\mathbb{R}^{d_c + d_{sp} + 1}$), the only solution to the system is $\bar{\mathbf{w}}_c = \mathbf{0}, \mathbf{w}_{sp} = \mathbf{0}$, proving the last part of our statement.

Moving forward to demand multiple calibration on second moments $\mathbb{E}[Y^2 \mid f(X)_1 = \alpha, E = e_i] = \mathbb{E}[Y^2 \mid f(X)_1 = \alpha, E = e_j]$ for all $i, j \in [k]$, we may write this as:

$$\sigma_{y,i}^2 - \frac{\sigma_{f,y,i}^2}{\sigma_{f,i}^2} = \sigma_{y,j}^2 - \frac{\sigma_{f,y,j}^2}{\sigma_{f,j}^2} \quad \forall i, j \in [k].$$

Plugging Equation (10) into the above, a simplified expression is obtained:

$$\sigma_{y,i}^2 - t\sigma_{f,y,i}^2 = \sigma_{y,j}^2 - t\sigma_{f,y,j}^2 \quad \forall i, j \in [k].$$

Again we can divide by t and obtain an explicit expression using $\bar{\mathbf{w}}_c, \mathbf{w}_{sp}$:

$$\bar{\mathbf{w}}_c^\top \Sigma_i^c \mathbf{w}_c^* - (\mathbf{w}_c^{*\top} \Sigma_i^c \mathbf{w}_c^* + \sigma_y^2) \mathbf{w}_{sp}^\top \mu_i = \bar{\mathbf{w}}_c^\top \Sigma_j^c \mathbf{w}_c^* - (\mathbf{w}_c^{*\top} \Sigma_j^c \mathbf{w}_c^* + \sigma_y^2) \mathbf{w}_{sp}^\top \mu_j \quad \forall i, j \in [k].$$

Finally, we can plug in Equation (11) and introduce another variable $t_3 \in \mathbb{R}$ to turn the above equations into:

$$\bar{\mathbf{w}}_c^\top \left(\Sigma_i^c \mathbf{w}_c^* + \left(\frac{\mathbf{w}_c^{*\top} \Sigma_i^c \mathbf{w}_c^* + \sigma_y^2}{\mathbf{w}_c^{*\top} \mu_i^c} \right) \mu_i^c \right) + t_2 \left(\frac{\mathbf{w}_c^{*\top} \Sigma_i^c \mathbf{w}_c^*}{\mathbf{w}_c^{*\top} \mu_i^c} \right) + t_3 = 0.$$

It is now easy to see that if $k > d_c + 2$ and $\mathbf{M}_2(\{\mu_i, \Sigma_i\}_{i=1}^k, \sigma_y^2, \mathbf{w}_c^*)$ has full rank, the only solution to these equations satisfies $\bar{\mathbf{w}}_c = \mathbf{0}, t_2 = t_3 = 0$. When this is plugged into Equation (11), we find that if $k > d_{sp}$ and the spurious means span $\mathbb{R}^{d_{sp}}$ then the only possible solution is $\mathbf{w}_{sp} = \mathbf{0}$. Finally, $\bar{\mathbf{w}}_c = \mathbf{0}$ means $\mathbf{w}_c^* = t\mathbf{w}_c$, and if $f(\mathbf{x})$ is calibrated then we must have $t = 1$ since otherwise its estimate of the conditional mean is incorrect. Hence our proof is concluded. \blacksquare

B Dataset Statistics and Models

For each of the five WILDS experiments presented in Section 6, we briefly describe the data and report the splits we use for training, validation and test. In each experiment we train a model on the training set, and the calibrators on the validation set. We then compare all alternatives (Original, Naive Calibration and Robust Calibration) on the held-out test set (OOD). Whenever an In-Domain (ID) test set is available (*PovertyMap*, *Camelyon17* and *AmazonReviews*), we evaluate the model on it as well.

B.1 PovertyMap

Problem Setting *PovertyMap* is a regression task of poverty mapping across countries. Input \mathbf{x} is a multispectral satellite image, output y is a real-valued asset wealth index and domain d is a country and whether the satellite image is of an urban or a rural area. The goal is to generalize across countries and demonstrate subpopulation performance across urban and rural areas.

Data *PovertyMap* is based on a dataset collected by [48], which organized satellite images and survey data from 23 African countries between 2009 and 2016. There are 23 countries, and every location is classified as either urban or rural. Each example includes the survey year, and its urban/rural classification.

1. Training: 10000 images from 13 countries.
2. Validation (OOD): 4000 images from 5 different countries (distinct from training and test (OOD) countries).
3. Test (OOD): 4000 images from 5 different countries (distinct from training and validation (OOD) countries).
4. Validation (ID): 1000 images from the same 13 countries in the training set.
5. Test (ID): 1000 images from the same 13 countries in the training set.

B.2 *Camelyon17*

Problem Setting *Camelyon17* is a tumor identification task across different hospitals. Input x is an histopathological image, label y is a binary indicator of whether the central region contains any tumor tissue and domain d is an integer identifying the hospital. The training and validation sets include the same four hospitals, and the goal is to generalize to an unseen fifth hospital.

Data The dataset comprises 450000 patches extracted from 50 whole-slide images (WSIs) of breast cancer metastases in lymph node sections, with 10 WSIs from each of five hospitals in the Netherlands [2]. Each WSI was manually annotated with tumor regions by pathologists, and the resulting segmentation masks were used to determine the labels for each patch. Data is split according to the hospital from which patches were taken.

1. Training: 335996 patches taken from each of the 4 hospitals in the training set.
2. Validation: 60000 patches taken from each of the 4 hospitals in the training set (15000 patches from each hospital).
3. Test (OOD): 85054 patches taken from the 5th hospital, which was chosen because its patches were the most visually distinctive.

B.3 *CivilComments*

Problem Setting *CivilComments* is a toxicity classification task across different demographic identities. Input x is a comment on an online article, label y indicates if it is toxic, and domain d is a one-hot vector with 8 dimensions corresponding to whether the comment mentions either of the 8 demographic identities *male*, *female*, *LGBTQ*, *Christian*, *Muslim*, *other religions*, *Black*, and *White*. The goal is to do well across all subpopulations, as computed through the average and worst case model performance.

Data *CivilComments* comprises 450000 comments, annotated for toxicity and demographic mentions by multiple crowdworkers, where toxicity classification is modeled as a binary task [5]. Each comment was originally made on an online article. Articles are randomly partitioned into disjoint training, validation, and test splits, and then formed the corresponding datasets by taking all comments on the articles in those splits.

1. Training: 269038 comments.
2. Validation: 45180 comments.
3. Test: 133782 comments.

B.4 *FMoW*

Problem Setting *FMoW* is a building and land multi-class classification task across regions and years. Input x is an RGB satellite image, label y is one of 62 building or land use categories, and domain d is the time the image was taken and the geographical region it captures. The goal is to generalize across time, and improve subpopulation performance across all regions.

Data *FMoW* is based on the Functional Map of the World dataset [7], which includes over 1 million high-resolution satellite images from over 200 countries, based on the functional purpose of the buildings or land in the image, over the years 2002–2018. We use a subset of this data introduced in [23], which is split into three time range domains, 2002–2013, 2013–2016, and 2016–2018, as well as five geographical regions as subpopulations: *Africa*, *Americas*, *Oceania*, *Asia* and *Europe*.

1. Training: 76863 images from the years 2002–2013.
2. Validation (OOD): 19915 images from the years from 2013–2016.
3. Test (OOD): 22108 images from the years from 2016–2018.
4. Validation (ID): 11483 images from the years from 2002–2013.
5. Test (ID): 11327 images from the years from 2002–2013.

B.5 AmazonReviews

Problem Setting Amazon Reviews is a sentiment classification task across multiple product areas. Input x is the text of a product review on Amazon, label y is the binarized star rating (1 for an above 3 starred review and 0 for below) for that review, and domain d is the product domain. The objective is to generalize to new product domains that are not represented in the training set.

Data The dataset is a modified version of the Amazon Reviews dataset [31] that originally includes 1.4 million reviews on Amazon. We randomly choose six domains and extract a balanced set from each, containing 14000 examples for every domain (84000 in total). The domains chosen are: *Digital Music* (DM), *Beauty* (B), *Amazon Instant Video* (AIV), *Video Games* (VG), *Musical Instruments* (MI), *Sports and Outdoors* (SAO). To measure generalization to unseen product domains, we train on reviews from five different product areas and test performance on another, previously unseen product area. We perform this experiment six times, changing in each iteration the held-out product area domain.

1. Training: 50000 reviews from 5 domains (10000 each)
2. Validation (ID): 10000 reviews from the same 5 domains as in training (2000 each)
3. Test (ID): 10000 reviews from the same 5 domains as in training (2000 each)
4. Test (OOD): 10000 reviews from a 6th product area, distinct from the 5 product areas used in training, validation and in-domain test sets.

Models In the following we briefly describe each of the models used in the experiments reported in Section 7.

- **BERT** - BERT is a 12-layer Transformer model [46] that represents textual inputs contextually and sequentially [10]. It is widely used in NLP, and is considered the standard benchmark for any state-of-the-art system. It was previously shown to be miscalibrated across its training and test environments [9]. In our *CivilComments* experiments, we use BERT-base-uncased, a smaller variant of BERT which has a layer size of 768
- **DenseNet** - Dense Convolutional Network (DenseNet), is a feed-forward neural network where for each layer, the feature-maps of all preceding layers are used as inputs, and its own feature-maps are used as inputs into all subsequent layers [20]. DenseNets are widely used in computer vision, especially for image classification tasks. We use a DenseNet-121 model, a DenseNet variant with 121 layers, in the *Camelyon17* and *FMoW* experiments.
- **ResNet** - Residual Network (ResNet) is a feed-forward neural network where layers are reformulated to learning residual functions with reference to the layer inputs [16]. DenseNets were shown to be successful in multiple image recognition tasks. We use the 18-layer variant, ResNet-18, in the *PovertyMap* experiment.
- **Random Forest** - Random forest is an ensemble learning method that constructs many decision trees and averages across them [6]. It is commonly used as a baseline in NLP [34]. While there better models for text classification, it is an interesting model that often performs well on in-domain benchmarks even though it has known calibration issues. In our *AmazonReviews* experiments, we train a Random Forest model, alongside a Logistic Regression and a Naive Bayes, using a TFIDF text representation. In the supplementary materials we report additional results with the different models.

We run our models using the default setting used in [23]. Each model is trained four times, using a different random seed at each run. We report performance averages and their standard deviation in Section 7.

Training Algorithms In the WILDS experiments, for each dataset we train our models using three out of these four alternatives:

- **ERM** - Empirical risk minimization (ERM) is a training algorithm that looks for models that minimize the average training loss, regardless of the training environment.
- **IRM** Invariant risk minimization (IRM) [1] is a training algorithm that penalizes feature distributions that have different optimal linear classifiers for each environment.

- **DeepCORAL** DeepCORAL [45] is an algorithm that penalizes differences in the means and covariances of the feature distributions for each training environment. It was originally proposed in the context of domain adaptation, and has been subsequently adapted for domain generalization [12].
- **GroupDRO** - Group DRO [19] uses distributionally robust optimization (DRO) to explicitly minimize the loss on the worst-case environment.

We do not perform any hyperparameter search, and use the default version available in [23].

C Additional Results - Alternative Models on *AmazonReviews*

Target Domain	ID	OOD		
		Orig.	Naive Cal.	Rob. Cal.
<i>DM</i>	0.837	0.729	0.725	0.726
<i>B</i>	0.836	0.809	0.813	0.818
<i>AV</i>	0.822	0.79	0.783	0.799
<i>VG</i>	0.822	0.764	0.779	0.784
<i>MI</i>	0.833	0.913	0.903	0.893
<i>SAO</i>	0.838	0.782	0.795	0.796

Table S1: Accuracy on *AmazonReviews*, where a Logistic Regression model is trained on five domains and tested on an unseen target.

Target Domain	ID	OOD		
		Orig.	Naive Cal.	Rob. Cal.
<i>DM</i>	0.796	0.751	0.764	0.752
<i>B</i>	0.786	0.775	0.737	0.77
<i>AV</i>	0.796	0.77	0.781	0.77
<i>VG</i>	0.788	0.708	0.796	0.787
<i>MI</i>	0.793	0.825	0.883	0.874
<i>SAO</i>	0.693	0.561	0.775	0.75

Table S2: Accuracy on *AmazonReviews*, where a Naive Bayes model is trained on five domains and tested on an unseen target.

In Section 7 in the paper, we report the results of a Random Forest classifier on the *AmazonReviews* dataset. Additionally, We have performed the same experiment with alternative models. In Tables S1 and S2, we report the results of two other models, Logistic Regression and Naive Bayes, respectively.